

Study of Decay Mechanisms in $B^- \rightarrow \Lambda_c^+ \bar{p} \pi^-$ Decays and Observation of Low-Mass Structure in the $\Lambda_c^+ \bar{p}$ System

N. Gabyshev,¹ K. Abe,⁸ K. Abe,⁴⁰ I. Adachi,⁸ H. Aihara,⁴² Y. Asano,⁴⁶ V. Aulchenko,¹ T. Aushev,¹² A. M. Bakich,³⁷ U. Bitenc,¹³ I. Bizjak,¹³ S. Blyth,²⁵ A. Bondar,¹ A. Bozek,²⁶ M. Bračko,^{8,19,13} J. Brodzicka,²⁶ T. E. Browder,⁷ P. Chang,²⁵ Y. Chao,²⁵ A. Chen,²³ W. T. Chen,²³ B. G. Cheon,³ R. Chistov,¹² S.-K. Choi,⁶ Y. Choi,³⁶ A. Chuvikov,³³ S. Cole,³⁷ J. Dalseno,²⁰ M. Danilov,¹² M. Dash,⁴⁷ A. Drutskoy,⁴ S. Eidelman,¹ Y. Enari,²¹ S. Fratina,¹³ T. Gershon,⁸ G. Gokhroo,³⁸ B. Golob,^{18,13} A. Gorišek,¹³ T. Hara,³⁰ H. Hayashii,²² M. Hazumi,⁸ T. Hokuue,²¹ Y. Hoshi,⁴⁰ S. Hou,²³ W.-S. Hou,²⁵ Y. B. Hsiung,²⁵ T. Iijima,²¹ A. Imoto,²² K. Inami,²¹ A. Ishikawa,⁸ R. Itoh,⁸ M. Iwasaki,⁴² Y. Iwasaki,⁸ J. H. Kang,⁴⁸ J. S. Kang,¹⁵ S. U. Kataoka,²² N. Katayama,⁸ H. Kawai,² T. Kawasaki,²⁸ H. R. Khan,⁴³ H. Kichimi,⁸ H. J. Kim,¹⁶ H. O. Kim,³⁶ S. K. Kim,³⁵ S. M. Kim,³⁶ K. Kinoshita,⁴ S. Korpar,^{19,13} P. Krokovny,¹ S. Kumar,³¹ C. C. Kuo,²³ A. Kuzmin,¹ Y.-J. Kwon,⁴⁸ J. S. Lange,⁵ G. Leder,¹¹ T. Lesiak,²⁶ S.-W. Lin,²⁵ F. Mandl,¹¹ T. Matsumoto,⁴⁴ Y. Mikami,⁴¹ W. Mitaroff,¹¹ H. Miyake,³⁰ H. Miyata,²⁸ R. Mizuk,¹² T. Nagamine,⁴¹ Y. Nagasaka,⁹ E. Nakano,²⁹ M. Nakao,⁸ H. Nakazawa,⁸ Z. Natkaniec,²⁶ S. Nishida,⁸ O. Nitoh,⁴⁵ S. Ogawa,³⁹ T. Ohshima,²¹ T. Okabe,²¹ S. Okuno,¹⁴ S. L. Olsen,⁷ Y. Onuki,²⁸ H. Ozaki,⁸ H. Palka,²⁶ C. W. Park,³⁶ H. Park,¹⁶ N. Parslow,³⁷ L. S. Peak,³⁷ R. Pestotnik,¹³ L. E. Piilonen,⁴⁷ M. Rozanska,²⁶ H. Sagawa,⁸ Y. Sakai,⁸ N. Sato,²¹ T. Schietinger,¹⁷ O. Schneider,¹⁷ A. J. Schwartz,⁴ K. Senyo,²¹ R. Seuster,⁷ M. E. Sevior,²⁰ H. Shibuya,³⁹ V. Sidorov,¹ J. B. Singh,³¹ A. Somov,⁴ R. Stamen,⁸ S. Stanič,^{46,*} M. Starič,¹³ T. Sumiyoshi,⁴⁴ S. Y. Suzuki,⁸ O. Tajima,⁸ F. Takasaki,⁸ K. Tamai,⁸ N. Tamura,²⁸ M. Tanaka,⁸ Y. Teramoto,²⁹ X. C. Tian,³² T. Tsuboyama,⁸ T. Tsukamoto,⁸ S. Uehara,⁸ T. Uglov,¹² K. Ueno,²⁵ S. Uno,⁸ P. Urquijo,²⁰ G. Varner,⁷ K. E. Varvell,³⁷ S. Villa,¹⁷ C. H. Wang,²⁴ M.-Z. Wang,²⁵ Q. L. Xie,¹⁰ B. D. Yabsley,⁴⁷ A. Yamaguchi,⁴¹ H. Yamamoto,⁴¹ Y. Yamashita,²⁷ M. Yamauchi,⁸ Heyoung Yang,³⁵ C. C. Zhang,¹⁰ J. Zhang,⁸ L. M. Zhang,³⁴ Z. P. Zhang,³⁴ V. Zhilich,¹ and D. Žontar^{18,13}

(Belle Collaboration)

¹*Budker Institute of Nuclear Physics, Novosibirsk*

²*Chiba University, Chiba*

³*Chonnam National University, Kwangju*

⁴*University of Cincinnati, Cincinnati, Ohio 45221*

⁵*University of Frankfurt, Frankfurt*

⁶*Gyeongsang National University, Chinju*

⁷*University of Hawaii, Honolulu, Hawaii 96822*

⁸*High Energy Accelerator Research Organization (KEK), Tsukuba*

⁹*Hiroshima Institute of Technology, Hiroshima*

¹⁰*Institute of High Energy Physics, Chinese Academy of Sciences, Beijing*

¹¹*Institute of High Energy Physics, Vienna*

¹²*Institute for Theoretical and Experimental Physics, Moscow*

¹³*J. Stefan Institute, Ljubljana*

¹⁴*Kanagawa University, Yokohama*

¹⁵*Korea University, Seoul*

¹⁶*Kyungpook National University, Taegu*

¹⁷*Swiss Federal Institute of Technology of Lausanne, EPFL, Lausanne*

¹⁸*University of Ljubljana, Ljubljana*

¹⁹*University of Maribor, Maribor*

²⁰*University of Melbourne, Victoria*

²¹*Nagoya University, Nagoya*

²²*Nara Women's University, Nara*

²³*National Central University, Chung-li*

²⁴*National United University, Miao Li*

²⁵*Department of Physics, National Taiwan University, Taipei*

²⁶*H. Niewodniczanski Institute of Nuclear Physics, Krakow*

²⁷*Nihon Dental College, Niigata*

²⁸*Niigata University, Niigata*

²⁹*Osaka City University, Osaka*

³⁰*Osaka University, Osaka*

³¹*Panjab University, Chandigarh*

³²Peking University, Beijing³³Princeton University, Princeton, New Jersey 08544³⁴University of Science and Technology of China, Hefei³⁵Seoul National University, Seoul³⁶Sungkyunkwan University, Suwon³⁷University of Sydney, Sydney NSW³⁸Tata Institute of Fundamental Research, Bombay³⁹Toho University, Funabashi⁴⁰Tohoku Gakuin University, Tagajo⁴¹Tohoku University, Sendai⁴²Department of Physics, University of Tokyo, Tokyo⁴³Tokyo Institute of Technology, Tokyo⁴⁴Tokyo Metropolitan University, Tokyo⁴⁵Tokyo University of Agriculture and Technology, Tokyo⁴⁶University of Tsukuba, Tsukuba⁴⁷Virginia Polytechnic Institute and State University, Blacksburg, Virginia 24061⁴⁸Yonsei University, Seoul

(Received 3 June 2005; published 11 December 2006)

Using a sample of $152 \times 10^6 B\bar{B}$ pairs accumulated with the Belle detector at the KEKB e^+e^- collider, we study the decay mechanism of three-body charmed decay $B^- \rightarrow \Lambda_c^+ \bar{p} \pi^-$. The intermediate two-body decay $B^- \rightarrow \Sigma_c(2455)^0 \bar{p}$ is observed for the first time with a branching fraction of $(3.7 \pm 0.7 \pm 0.4 \pm 1.0) \times 10^{-5}$ and a statistical significance of 8.4σ . We also observe a low-mass enhancement in the $(\Lambda_c^+ \bar{p})$ system, which can be parametrized as a Breit-Wigner function with a mass of $(3.35_{-0.02}^{+0.01} \pm 0.02)$ GeV/ c^2 and a width of $(0.07_{-0.03}^{+0.04} \pm 0.04)$ GeV/ c^2 . We measure its branching fraction to be $(3.9_{-0.7}^{+0.8} \pm 0.4 \pm 1.0) \times 10^{-5}$ with a statistical significance of 6.2σ . The errors are statistical, systematic, and that of the $\Lambda_c^+ \rightarrow pK^- \pi^+$ decay branching fraction.

DOI: 10.1103/PhysRevLett.97.242001

PACS numbers: 13.25.Hw, 14.20.Lq

Recently three-body baryon production in charmless B decays has been studied with the Belle detector [1–4]. Analysis of these decays shows a common feature: the invariant mass of the baryon-antibaryon system is peaked near threshold. This feature has generated much theoretical discussion and may be due to a fragmentation effect, production of resonances near threshold, or final state interaction of the produced baryon-antibaryon system [5–9]. It is of interest to learn whether similar behavior is also observed in B decays to charmed baryons. The three-body decay $B^- \rightarrow \Lambda_c^+ \bar{p} \pi^-$ has been previously studied at CLEO [10] and Belle [11] with 9.2 fb^{-1} and 29.1 fb^{-1} of data, respectively. Here we report analysis of the $B^- \rightarrow \Lambda_c^+ \bar{p} \pi^-$ decay on a Dalitz plane based on a data sample of 140 fb^{-1} accumulated at the $\Upsilon(4S)$ resonance with the Belle detector at the KEKB e^+e^- collider [12].

The large-solid-angle magnetic spectrometer Belle described in detail elsewhere [13] consists of a three-layer silicon vertex detector (SVD), a 50-layer cylindrical drift chamber (CDC), a mosaic of aerogel threshold Čerenkov counters (ACC), a barrel-like array of time-of-flight scintillation counters (TOF), and an array of CsI(Tl) crystals (ECL) located inside a superconducting coil providing a 1.5 T magnetic field. An iron flux return located outside the coil is instrumented to detect muons and K_L^0 mesons (KLM). We use a GEANT based Monte Carlo (MC) simulation to model the response of the detector and determine its acceptance [14].

The event selection is based on track information from the SVD and CDC and particle identification (PID) from the combined response of the CDC, ACC, and TOF. We require the impact parameters of all primary tracks with respect to the interaction point (IP) to be within ± 1 cm in the transverse (x - y) plane and within ± 5 cm in the z direction (opposite to the e^+ beam). Proton, kaon, and pion candidates are selected using $p/K/\pi$ likelihood functions provided by the PID system. We require the likelihood ratios $L_i/(L_i + L_j)$ to be greater than 0.6, where the subscript i denotes the selected particle and j the other two particle species. The PID efficiency is 98% for each track, and the fake probability of a pion (kaon) to be identified as a kaon (pion) is less than 5%. The probability for a pion or kaon to be identified as a proton is less than 2%. We detect the Λ_c^+ via five decay modes: $\Lambda_c^+ \rightarrow pK^- \pi^+$, $p\bar{K}^0$, $\Lambda\pi^+$, $p\bar{K}^0\pi^+\pi^-$, and $\Lambda\pi^+\pi^+\pi^-$. Inclusion of charge conjugate states is implicit unless otherwise stated. Neutral kaons and Λ baryons are reconstructed in the $K_S^0 \rightarrow \pi^+\pi^-$ and $\Lambda \rightarrow p\pi^-$ decay, respectively. The $B^- \rightarrow \Lambda_c^+ \bar{p} \pi^-$ events are identified by their energy difference $\Delta E = (\sum E_i) - E_{\text{beam}}$, and the beam-energy constrained mass $M_{\text{bc}} = \sqrt{E_{\text{beam}}^2 - (\sum \vec{p}_i)^2}$, where E_{beam} is the beam energy, and \vec{p}_i and E_i are the three-momenta and energies of the B meson decay products, all defined in the e^+e^- center-of-mass system. To suppress continuum background, we impose requirements on the angle between

the thrust axis of the B candidate tracks and that of the other tracks and on the ratio of the second to the zeroth Fox-Wolfram moments [15].

Figure 1 shows the ΔE distribution for $M_{bc} > 5.27 \text{ GeV}/c^2$ for the selected B candidates. The signal yield is extracted by a fit to the ΔE distribution, as it is free from combinatorial backgrounds from other B decays. The fit uses a Gaussian for the signal fixed to MC data and a third-order polynomial for the background for which a MC study shows a broad background below the signal due to continuum events and combinatorial backgrounds from other B decays, such as $\bar{B}^0 \rightarrow \Lambda_c^+ \bar{p} \pi^0$. We obtain 264 ± 20 signal events with a statistical significance of 17.1σ . The uncertainty due to the background parameterization is estimated by repeating the fit with first and third order polynomials and found to be small (1.5%). The significance is defined as $\sqrt{-2 \ln(\mathcal{L}_0/\mathcal{L}_{\max})}$, where \mathcal{L}_{\max} and \mathcal{L}_0 denote the maximum likelihoods with the fitted signal yield and the yield fixed at zero, respectively.

Figure 2(a) shows the $M(\Lambda_c^+ \pi^-)$ distribution, where clear signals are seen from the intermediate two-body $B^- \rightarrow \Sigma_c(2455/2520)^0 \bar{p}$ decay [10,11]. The open histogram is the distribution from the B signal region ($|\Delta E| < 0.03 \text{ GeV}$ and $M_{bc} > 5.27 \text{ GeV}/c^2$). The hatched histogram is the distribution from sideband regions ($-0.10 \text{ GeV} < \Delta E < -0.04 \text{ GeV}$ or $0.04 \text{ GeV} < \Delta E < 0.20 \text{ GeV}$) normalized to the B signal region area. The curve shows the result of the fit, which includes the contribution from $\Sigma_c(2455/2520)^0 \rightarrow \Lambda_c^+ \pi^-$ decays and the background parametrized with a linear function. The $\Sigma_c(2455/2520)^0$ signal shapes are fixed from MC calculations assuming a Breit-Wigner function convolved with the resolution function and using $\Sigma_c(2455/2520)^0$ masses and widths from Ref. [16]. To extract the yields for $B^- \rightarrow \Sigma_c(2455/2520)^0 \bar{p}$ decays, background from continuum and/or other B decays is taken into account by fitting simultaneously the B signal and sideband regions in the ΔE distribution. From the fit, we obtain $35.3^{+6.4}_{-6.0}$ signal events with a statistical significance of 8.2σ for the $B^- \rightarrow \Sigma_c(2455)^0 \bar{p}$ decay, and $12.6^{+5.4}_{-4.7}$ signal events with a statistical significance of 3.0σ for the $B^- \rightarrow \Sigma_c(2520)^0 \bar{p}$ decay.

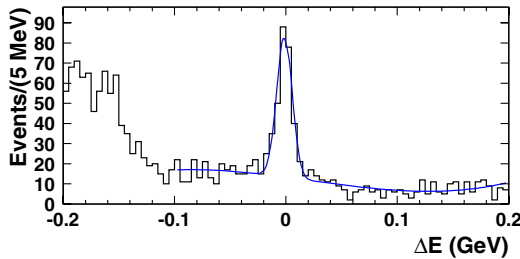


FIG. 1 (color online). ΔE distribution for $M_{bc} > 5.27 \text{ GeV}/c^2$ for $B^- \rightarrow \Lambda_c^+ \bar{p} \pi^-$ candidates. The curve shows the result of the fit.

Figure 2(b) shows the $M(\bar{p} \pi^-)$ distribution for the $B^- \rightarrow \Lambda_c^+ \bar{p} \pi^-$ candidate events from fits to the ΔE distribution in 100 MeV bins of $(\bar{p} \pi^-)$ mass with constraints of $M(\Lambda_c^+ \pi^-) > 2.6 \text{ GeV}/c^2$ to remove Σ_c^0 intermediate states and $M(\Lambda_c^+ \bar{p}) > 3.5 \text{ GeV}/c^2$ to remove an enhancement at low $(\Lambda_c^+ \bar{p})$, which is discussed below. The histogram shows the result of a fit including the following contributions: three-body phase space, $B^- \rightarrow \Lambda_c^+ \bar{\Delta}(1232)^-$ [17], and two other contributions, with parameters close to the $\Delta(1600)$ and $\Delta(2420)$ resonances tentatively referred to as $\Delta_X(1600)$ and $\Delta_X(2420)$. The signal shapes are fixed from the MC calculations. Both three-body phase space and $\Delta(1232)$ contributions have a 0.5σ significance. The statistical significance of the $\Delta_X(1600)$ contribution is 6.7σ with a yield of 82 ± 12 events while that of the $\Delta_X(2420)$ is 4.7σ with a yield of 41 ± 9 events.

Figure 2(c) shows the $M(\Lambda_c^+ \bar{p})$ distribution for $B^- \rightarrow \Lambda_c^+ \bar{p} \pi^-$ decay candidate events from fits to the ΔE distribution in 50 MeV bins of $(\Lambda_c^+ \bar{p})$ mass with

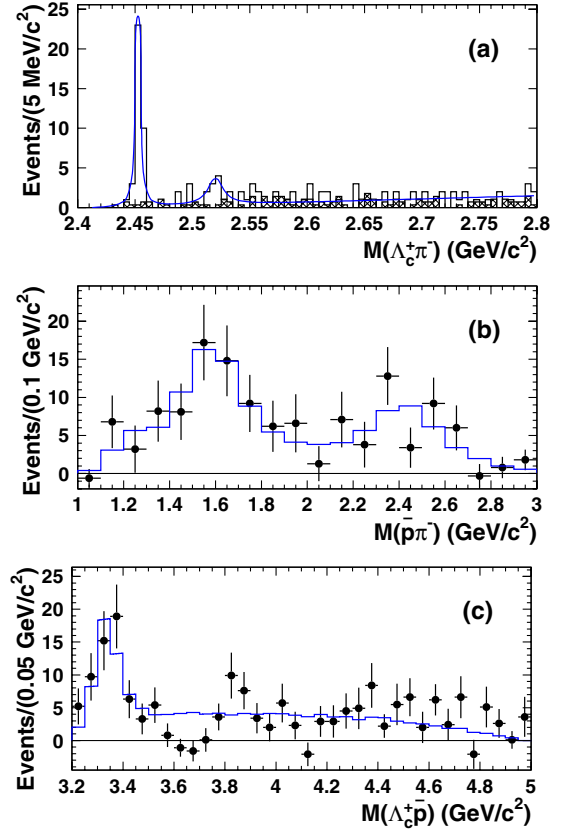


FIG. 2 (color online). (a) $M(\Lambda_c^+ \pi^-)$ distribution for the B signal region (open histogram) and fit results (curve); the distribution in the sidebands is also shown (hatched). (b),(c) B^- yields (points) from fits to ΔE distributions, (b) in bins of $M(\bar{p} \pi^-)$, requiring $M(\Lambda_c^+ \pi^-) > 2.6 \text{ GeV}/c^2$ and $M(\Lambda_c^+ \bar{p}) > 3.5 \text{ GeV}/c^2$; and (c) in bins of $M(\Lambda_c^+ \bar{p})$, requiring $M(\Lambda_c^+ \pi^-) > 2.6 \text{ GeV}/c^2$ and $M(\bar{p} \pi^-) > 1.6 \text{ GeV}/c^2$. The histograms show fit results, see the text.

$M(\Lambda_c^+ \pi^-) > 2.6 \text{ GeV}/c^2$ to remove Σ_c contributions and $M(\bar{p}\pi^-) > 1.6 \text{ GeV}/c^2$ to remove low $(\bar{p}\pi^-)$ masses. A low-mass enhancement is observed. The histogram is the result of a fit parameterizing the distribution with a Breit-Wigner peak and feed-downs from the $B^- \rightarrow \Lambda_c^+ \bar{\Delta}_X(1600/2420)^{--}$ contributions. This fit gives a mass of $(3.35_{-0.02}^{+0.01}) \text{ GeV}/c^2$ and full width of $(0.07_{-0.03}^{+0.04}) \text{ GeV}/c^2$. The fit yield is 50 ± 10 events with a statistical significance of 5.6σ . A second peak near $3.8 \text{ GeV}/c^2$ has a mass of $(3.84 \pm 0.01) \text{ GeV}/c^2$ and width of $(0.03 \pm 0.03) \text{ GeV}/c^2$. The yield of this peak is 15 ± 6 events (2.8σ) and not studied any further.

Systematic uncertainties are estimated by performing fits with different background parameterizations including the contributions of the $B^- \rightarrow \Lambda_c^+ \bar{\Delta}_X(1600/2420)^{--}$ feed-downs with a free number of events or a broad Breit-Wigner function with and without the second peak at $3.8 \text{ GeV}/c^2$. The mass variation is less than $0.02 \text{ GeV}/c^2$, and the width varies by less than $0.04 \text{ GeV}/c^2$.

For the $(\Lambda_c^+ \bar{p})$ structure, we studied the distribution of the helicity angle, $\Theta(\Lambda_c^+ \bar{p})$, defined as the angle between the Λ_c^+ momentum and the direction opposite to the B meson momentum in the $(\Lambda_c^+ \bar{p})$ rest frame. If the $(\Lambda_c^+ \bar{p})$ structure is due to fragmentation, the distribution will be asymmetric, while for a resonance it will be symmetric [8] and could provide information on the spin of the $(\Lambda_c^+ \bar{p})$ state. Figure 3 shows the efficiency corrected helicity distribution for this decay for events from the region $M(\Lambda_c^+ \bar{p}) < 3.6 \text{ GeV}/c^2$, where the data points were obtained from fits to the ΔE distributions. The data are consistent with the uniform distribution expected for a $J = 0$ state ($\chi^2/\text{ndf} = 0.97$). A fit of our data to a general formula for the angular distribution $(1 + \alpha \cos^2 \Theta(\Lambda_c^+ \bar{p}))$ for a $J = 1$ state [18,19] gives $\alpha = (-0.15 \pm 0.54)$ ($\chi^2/\text{ndf} = 1.12$), see the solid curve in Fig. 3. The observed helicity asymmetry is $\frac{N_+ - N_-}{N_+ + N_-} = 0.32 \pm 0.14$, where N_+ and N_- are the efficiency corrected numbers of events with $\cos \Theta(\Lambda_c^+ \bar{p}) > 0$ and < 0 , respectively. No definite conclusions can be drawn from the helicity studies with this statistics.

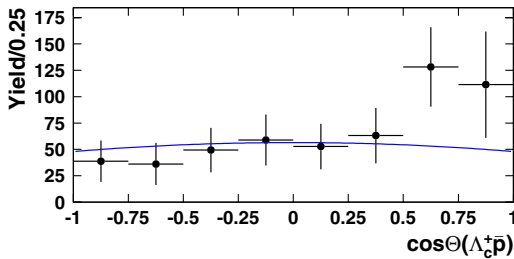


FIG. 3 (color online). The efficiency corrected helicity distribution for the $(\Lambda_c^+ \bar{p})$ structure. The solid line is the result of the fit to $[1 + \alpha \cos^2 \Theta(\Lambda_c^+ \bar{p})]$.

We determine the contributions from $\Sigma_c(2455/2520)$ and the low $(\Lambda_c^+ \bar{p})$ mass structure, taking into account cross talk between different resonant states and the variation of detection efficiency on the Dalitz plane. Figure 4 shows the Dalitz plot of $M(\bar{p}\pi^-)^2$ vs $M(\Lambda_c^+ \pi^-)^2$ for the events in the B signal region of $|\Delta E| < 0.03 \text{ GeV}$ and $M_{bc} > 5.27 \text{ GeV}/c^2$, where we estimate a background contamination of 37% in total. The Dalitz plot is subdivided into six regions corresponding to the six states discussed above: (1) $\Sigma_c(2455)^0 \bar{p} - M(\Lambda_c^+ \pi^-) < 2.48 \text{ GeV}/c^2$; (2) $\Sigma_c(2520)^0 \bar{p} - M(\Lambda_c^+ \pi^-) > 2.48 \text{ GeV}/c^2$ and $M(\Lambda_c^+ \pi^-) < 2.6 \text{ GeV}/c^2$; (3) $\Lambda_c^+ \bar{\Delta}(1232)^{--} - M(\Lambda_c^+ \pi^-) > 2.6 \text{ GeV}/c^2$ and $M(\bar{p}\pi^-) < 1.4 \text{ GeV}/c^2$; (4) $\Lambda_c^+ \bar{\Delta}_X(1600)^{--} - M(\Lambda_c^+ \pi^-) > 2.6 \text{ GeV}/c^2$, $M(\bar{p}\pi^-) > 1.4 \text{ GeV}/c^2$ and $M(\bar{p}\pi^-) < 2.0 \text{ GeV}/c^2$; (5) $\Lambda_c^+ \bar{\Delta}_X(2420)^{--} - M(\Lambda_c^+ \pi^-) > 2.6 \text{ GeV}/c^2$, $M(\bar{p}\pi^-) > 2.0 \text{ GeV}/c^2$ and $M(\Lambda_c^+ \bar{p}) > 3.6 \text{ GeV}/c^2$; (6) $(\Lambda_c^+ \bar{p})$ enhancement — $M(\bar{p}\pi^-) > 2.0 \text{ GeV}/c^2$ and $M(\Lambda_c^+ \bar{p}) < 3.6 \text{ GeV}/c^2$.

The resonance parameters are taken from [16]. The $(\Lambda_c^+ \bar{p})$ structure is represented as a Breit-Wigner function with mass $3.35 \text{ GeV}/c^2$ and full width $0.07 \text{ GeV}/c^2$, visible as a band in region 6 of Fig. 4. The B signal yield in the i th region is given as $X_i = \sum_{j=1}^6 \varepsilon_{ij} \cdot Y_j$, where ε_{ij} is the probability to reconstruct the j th intermediate state in the i th Dalitz plot region (estimated from the MC sample of j th state). We extract the signal Y_j from a simultaneous fit of the B signal yields X_i for the six ΔE distributions, where the width is fixed from MC data. Then, we calculate the branching fraction $\mathcal{B}_j = Y_j/[N_{BB} \times \eta \times \mathcal{B}(\Lambda_c^+ \rightarrow pK^- \pi^+)]$ for the j th intermediate state, combining the B signals tagged with the five Λ_c^+ decay modes. η is the

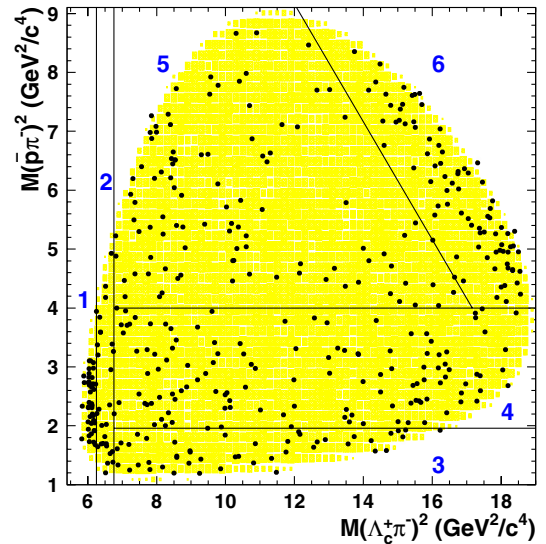


FIG. 4 (color online). The $M(\bar{p}\pi^-)^2$ vs $M(\Lambda_c^+ \pi^-)^2$ Dalitz plot subdivided into six regions. The points are the data in the B signal region. The shaded area is the phase space MC data.

TABLE I. Branching fractions for intermediate two-body states in $B^- \rightarrow \Lambda_c^+ \bar{p} \pi^-$ decay.

Mode	Yield (ev)	Significance (σ)	Efficiency (%)	Branching (10^{-5})	Interference error (10^{-5})
$B^- \rightarrow \Sigma_c(2455)^0 \bar{p}$	33_{-6}^{+7}	8.4	11.7	$3.7 \pm 0.7 \pm 0.4 \pm 1.0$	± 0.6
$B^- \rightarrow \Sigma_c(2520)^0 \bar{p}$	13_{-5}^{+6}	2.9	13.4	< 2.7 at 90% C.L.	± 0.8
$(\Lambda_c^+ \bar{p})$ structure	55_{-10}^{+11}	6.2	18.7	$3.9_{-0.7}^{+0.8} \pm 0.4 \pm 1.0$	± 2.1
$B^- \rightarrow \Lambda_c^+ \bar{\Delta}(1232)^{--}$	9_{-7}^{+8}	1.3	17.9	< 1.9 at 90% C.L.	± 0.8
$B^- \rightarrow \Lambda_c^+ \bar{\Delta}_X(1600)^{--}$	85_{-14}^{+15}	7.5	18.9	$5.9_{-1.0}^{+1.0} \pm 0.6 \pm 1.5$	± 4.7
$B^- \rightarrow \Lambda_c^+ \bar{\Delta}_X(2420)^{--}$	68_{-13}^{+15}	6.1	19.1	$4.7_{-0.9}^{+1.0} \pm 0.4 \pm 1.2$	± 4.5
$B^- \rightarrow \Lambda_c^+ \bar{p} \pi^-$	262 ± 20	18.1		$20.1 \pm 1.5 \pm 2.0 \pm 5.2$	

combined efficiency given by $\sum \eta_k \times \Gamma_k(\Lambda_c^+)/\Gamma(\Lambda_c^+ \rightarrow pK^- \pi^+)$ [16]. η_k is the efficiency of the B signal with the k th Λ_c^+ decay determined from MC calculations.

The resulting yields, branching fractions, and statistical significances for each intermediate state are listed in Table I. For the branching fractions, the first error is statistical and the second is systematic, whereas the third (26%) comes from the uncertainty in $\mathcal{B}(\Lambda_c^+ \rightarrow pK^- \pi^+)$.

Systematic uncertainties in the detection efficiencies arise from the track reconstruction efficiency (5%–7% depending on the process, assuming a correlated systematic error of about 1% per charged track); the PID efficiency (about 7% assuming a correlated systematic error of 2% per proton and 1% per pion or kaon), and MC statistics (1%–2%). The other uncertainties are associated with $\Gamma(\Lambda_c^+)/\Gamma(\Lambda_c^+ \rightarrow pK^- \pi^+)$ (1%–2%), the number of $B\bar{B}$ events (0.08%); and the parameters of the low mass ($\Lambda_c^+ \bar{p}$) enhancement, which can contribute up to 6% to the uncertainty of its branching fraction. The total systematic error is estimated to be 9%–11% depending on the intermediate state.

We estimate separately a possible effect of interference between the different observed intermediate states. Using special MC samples in which each of the relative phases among the six states is varied in steps of 90° , we compare the signal yield in individual regions of the Dalitz plot to that obtained using simulated events without any interference. The maximum deviation is treated as the uncertainty due to interference and is given in Table I. This simplified treatment of interference does not take into account a possibility of reduced compatibility between the simulated distributions with interference and data and indicates that the low-mass ($\Lambda_c^+ \bar{p}$) enhancement can be partially described by such an effect.

In summary, using a sample of 152×10^6 $B\bar{B}$ pairs, accumulated with the Belle detector at the KEKB collider, we performed an analysis on the Dalitz plane of the three-body charmed decay $B^- \rightarrow \Lambda_c^+ \bar{p} \pi^-$. We report first observation of the two-body decay mode $B^- \rightarrow \Sigma_c(2455)^0 \bar{p}$ and measure its branching fraction to be $(3.7 \pm 0.7 \pm 0.4 \pm 1.0) \times 10^{-5}$ with a statistical significance of 8.4σ .

We also observe a low-mass enhancement in the ($\Lambda_c^+ \bar{p}$) system, which can be parametrized as a Breit-Wigner function with a mass of $(3.35_{-0.02}^{+0.01} \pm 0.02)$ GeV/ c^2 and a width of $(0.07_{-0.03}^{+0.04} \pm 0.04)$ GeV/ c^2 . The branching fraction of the B^- decay to this structure is $(3.9_{-0.7}^{+0.8} \pm 0.4 \pm 1.0) \times 10^{-5}$ with a statistical significance of 6.2σ . The current data are not sufficient to determine an origin of this enhancement. The total three-body $B^- \rightarrow \Lambda_c^+ \bar{p} \pi^-$ decay branching fraction has been measured to be $(20.1 \pm 1.5 \pm 2.0 \pm 5.2) \times 10^{-5}$, which is consistent with previous results [10,11]. The branching fractions measurements supersede those in Ref. [11].

We thank the KEKB group for the excellent operation of the accelerator, the KEK cryogenics group for the efficient operation of the solenoid, and the KEK computer group and the NII for valuable computing and Super-SINET network support. We acknowledge support from MEXT and JSPS (Japan); ARC and DEST (Australia); NSFC (contract No. 10175071, China); DST (India); the BK21 program of MOEHRD and the CHEP SRC program of KOSEF (Korea); KBN (contract No. 2P03B 01324, Poland); MIST (Russia); MESS (Slovenia); NSC and MOE (Taiwan); and DOE (USA).

*On leave from Nova Gorica Polytechnic, Nova Gorica.

- [1] K. Abe *et al.* (Belle Collaboration), Phys. Rev. Lett. **88**, 181803 (2002).
- [2] K. Abe *et al.* (Belle Collaboration), Phys. Rev. Lett. **89**, 151802 (2002).
- [3] M.-Z. Wang *et al.* (Belle Collaboration), Phys. Rev. Lett. **90**, 201802 (2003).
- [4] M.-Z. Wang *et al.* (Belle Collaboration), Phys. Rev. Lett. **92**, 131801 (2004).
- [5] C. K. Chua, W. S. Hou, and S. Y. Tsai, Phys. Rev. D **66**, 054004 (2002).
- [6] H. Y. Cheng and K. C. Yang, Phys. Rev. D **66**, 094009 (2002).
- [7] C. K. Chua and W. S. Hou, Eur. Phys. J. C **29**, 27 (2003).
- [8] J. L. Rosner, Phys. Rev. D **68**, 014004 (2003).

- [9] B. Kerbikov, A. Stavinsky, and V. Fedotov, *Phys. Rev. C* **69**, 055205 (2004).
- [10] S. A. Dytman *et al.* (CLEO Collaboration), *Phys. Rev. D* **66**, 091101(R) (2002).
- [11] N. Gabyshev *et al.* (Belle Collaboration), *Phys. Rev. D* **66**, 091102(R) (2002).
- [12] S. Kurokawa and E. Kikutani, *Nucl. Instrum. Methods Phys. Res., Sect. A* **499**, 1 (2003).
- [13] A. Abashian *et al.* (Belle Collaboration), *Nucl. Instrum. Methods Phys. Res., Sect. A* **479**, 117 (2002).
- [14] R. Brun *et al.*, GEANT 3.21, CERN Report No. DD/EE/84-1, 1984. Events are generated with the CLEO group QQ program.
- [15] G. C. Fox and S. Wolfram, *Phys. Rev. Lett.* **41**, 1581 (1978).
- [16] S. Eidelman *et al.*, *Phys. Lett. B* **592**, 1 (2004).
- [17] H. Y. Cheng and K. C. Yang, *Phys. Rev. D* **67**, 034008 (2003).
- [18] F. Murgia and M. Melis, *Phys. Rev. D* **51**, 3487 (1995).
- [19] C. H. Wu *et al.* (Belle), *Phys. Rev. Lett.* **97**, 162003 (2006).